BEAM DYNAMICS AND DIAGNOSTICS FOR THE HIGH ENERGY BEAM TRANSPORT LINE OF MINERVA PROJECT AT SCK-CEN *

H. Kraft[†], L. Perrot, CNRS, Université Paris-Saclay, Université Paris Sud, IPN Orsay, France

Abstract

MYRRHA will be a research infrastructure highlighted by the first prototype of a sub-critical nuclear reactor driven by a 600 MeV particle accelerator (ADS). This project aims at exploring the transmutation of long-lived nuclear wastes. A first phase is planned to validate the reliability of a 100 MeV/4 mA Protons LINAC carrying the beam toward an ISOL facility, prefiguring the real MYRRHA demonstrator at 600 MeV [1]. This project is called MINERVA [2]. This paper presents the status of the beam dynamic studies for the high energy beam transport lines at 100 MeV. In agreement with the project requirements, we describe the specificities of these beam lines for which it is needed to implement a fast kicker-septum. This system will separate the beam between two main lines: toward the beam dump or the ISOL facility [3]. We also describe the studies on the Beam Position Monitor (BPM) selected for MYRRHA. Part of this work was support by the MYRTE project of the European Union [4].

INTRODUCTION

The high energy beam transport (HEBT) of MINERVA requires the construction of three beam lines. The first one named Energy Tuning Beam Dump (ETBD) line will be dedicated to the commissioning of the accelerator and during beam tuning phases. The beam will be stopped in a dedicated beam dump station (P_{max} = 400 kW). The second line named Full Power Beam Dump (FPBD) line will be in charge to ensure a full power reception of the beam on a dump installed in a dedicated area. This line will be connect the Protons Target Facility (PTF) line. This third line will be in charge to transport a given fraction of the Protons beam up to the building dedicated to nuclides production for irradiations, R&D and experimental physics. The FPBD line and the PTF line will have a common section and will be linked operationally. The beam transfer along the PTF line or the FPBD line will be provided using a kicker and septum (see Fig. 1). Moreover, the HEBT lines needs non-interceptive diagnostics to measure beam characteristics. Among them, Beam Position Monitor (BPM) are used to centre the beam. Beyond the beam position, devices allow us to measure beam energy, beam ellipticity and the beam current. This work describes the studies on the BPM selected for MINERVA, aiming to realise a parametric study and optimise the BPM sensitivity for a 100 MeV Proton beam.
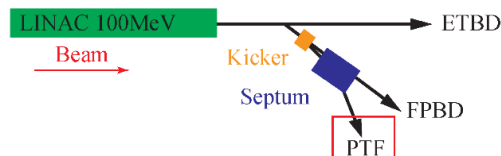

Figure 1: Scheme of the HEBT lines for MINERVA.

* Work supported by THALES AVS FRANCE SAS
† kraft@ipno.in2p3.fr

HEBT BEAM DYNAMIC

The HEBT beam dynamic studies are performed with the Tracewin software [5]. Allowing beam dynamics simulations and gradient's optimisation of the magnetic elements toward the beam lines as quadrupoles, dipoles, steerers. Adding statistical errors on the beam characteristics and the elements, an entire errors study can be achieved and has to fit with the beam requirements.

The nominal Protons beam characteristics along the HEBT will be 100 MeV at 4 mA. In the operating domain of the machine, the three beam lines can receive 400 kW maximum peak power. The maximum mean power in the beam lines will be: 400 W for the ETBD, 400 kW for FPBD, 50 kW for PTF. The mean power distributed along the lines can be monitored with the beam time structure suggested for the nominal operating mode at MINERVA (see Fig. 2).
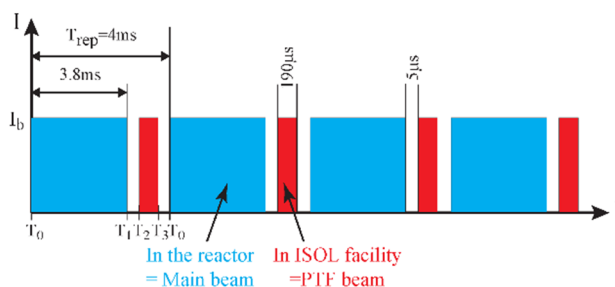

Figure 2: Beam time structure requirements for MINERVA in nominal operating mode.

A large fraction of the beam is transmitted to the FPBD, and periodically a fraction to the PTF. The bunch repetition rate of MYRRHA is 176 MHz (a bunch each 5.7 ns), leads a too short period of time to switch the beam between the two lines. In the low energy section of the LINAC, the chopper create holes in the time structure, expected in the range from 5 µs up to 20 µs. These holes allow the rise of field (T1 - T2), and the fall of field (T3 - T0), of a fast magnet aimed to bend the beam to the PTF line (see Fig. 2). As a fast dipole, it is planned to design a fast kicker magnet associated with a septum magnet.

Fast Magnet – Kicker & Septum

The kicker is activated in order to apply a short deviation to the beam going to the PTF section. A septum magnet must be installed in order to increase the beam deviation. Main characteristics of the kicker are presented in Table 1. The MYRRHA Kicker specifications are based on the existing CERN kicker build for CNAO [6].

Table 1: Specifications of the Kicker Magnet for the HEBT of MINERVA

Effective magnetic length (m)	0.6
Beam rigidity (T.m)	1.483
Maximum field (T)	0.0209
Deflection angle (mrad)	8.47
Aperture w x h (m²)	0.12 x 0.12
Nominal current for the max Field (A)	200
Maximum voltage (V)	2000
Number of turns N	10
Estimated inductance (µH)	75.4
Fall time = Rise time (µs)	12.6

The Septum magnet is a two parts element [7]. The first part is magnetic field free for the non-deviated beam going to the FPBD. The second part applies a stationary magnetic field at the beam going to the PTF. The two parts have to be separated with a «septum» along with a magnetic screen. The magnetic screen must be robust enough to resist strong mechanical stress from electromechanical forces. The septum characteristics are presented in Table 2. Specifications are based on the magnetic septa designed for MEDAUSTRON [8].

Table 2: Specifications of the Septum Magnet for the HEBT MYRRHA 100 MeV

Curvature radius (mm)	7420
Equivalent magnetic length (mm)	2022
Deflection angle (mrad)	273
Septum thickness + screen (mm)	10 + 1
Gap (mm)	120
Horizontal width in field (mm)	630
B nominal (Tesla)	0.2

The FPBD and PTF beam separation dynamic results are presented in Fig. 3. In common use, two quadrupoles are inserted after the kicker to ensure appropriate beam focusing. These quadrupoles are aligned along the FPBD beam axis. The beams are well separated and no power is deposited in the septum.
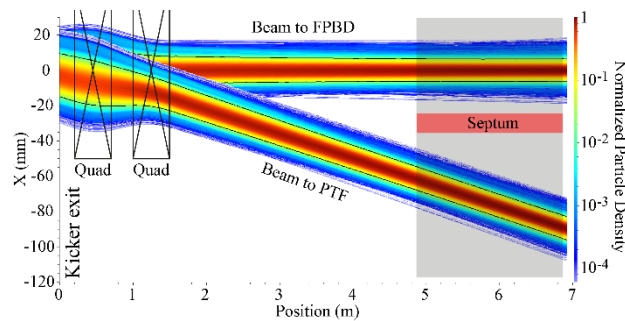

Figure 3: Horizontal beam density from the exit of the kicker up to the septum.

Beam Dynamic

Using the kicker and septum specifications, the beam dynamic along the PTF is calculated. Figure 4 shows the beam transverse envelop at 6 RMS.
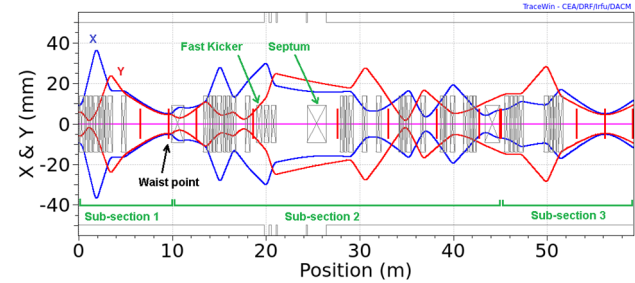

Figure 4: 6 RMS beam envelopes along the PTF line from the LINAC exit. In blue the horizontal plane (X), in red the vertical plane (Y).

The PTF line is structured in three sub-sections for the optics. The first one, connected to the LINAC, is common to all HEBT lines, adapting transversally the beam in order to obtain a well-known waist point. The second sub-section is a long right-right deviation section including the kicker-septum module. The third section is dedicated to the beam preparation for the PTF.

BEAM POSITION MONITOR

The BPM selected for MYRRHA is a button type electrostatic pick-up. This detector measure the charges induced by the electric field of the beam particles on an insulated metal plate [9]. For this purpose, four pick-up plates are mounted crosswise at the beam pipe wall. The beam position (centre-of-mass) is deduced with the difference signals of opposite plates for both transverse planes. This work yields to optimise the MYRRHA BPM of the HEBT, depending on the beam dynamic.

This work aims to realise a parametric study depending on BPM geometry and beam characteristics. The E-field can be estimated, for a Gaussian beam distribution, with the analytical approach in Eq. (1) and Eq. (2). This expression depends only to the beam characteristics:

$$\vec{E}(x,y,z) = \frac{\gamma e}{4\pi\varepsilon_o}\cdot\frac{N}{\sigma_x\sigma_y\sigma_z(2\pi)^{3/2}}\int\int\int_{Bd}f(x_p,y_p,z_p)dx_pdy_pdz_p \quad (1)$$

$$f(x_p,y_p,z_p) = \frac{e^{-\frac{1}{2}\left(\left(\frac{x_p}{\sigma_x}\right)^2+\left(\frac{y_p}{\sigma_y}\right)^2+\left(\frac{z_p}{\sigma_z}\right)^2\right)}}{(x-x_p)^2+(y-y_p)^2+(\gamma z-z_p)^2} \quad (2)$$

With γ the Lorentz factor, e elementary charge, ε$_0$ vacuum permittivity, N Protons number in the Bd distribution, $\sigma_{x,y,z}$ (∼ 2 mm) the RMS bunch sizes in x, y and z plane.

Figure 5 (a) shows the principle of a charges induction in the BPM. The induction effects of the electrostatic field on the pick-ups are calculated using the CST Wakefield solver [10]. Figure 5 (b) shows the electrostatic field emitted by the centered bunch in the longitudinal cut of the calculated BPM using CST.
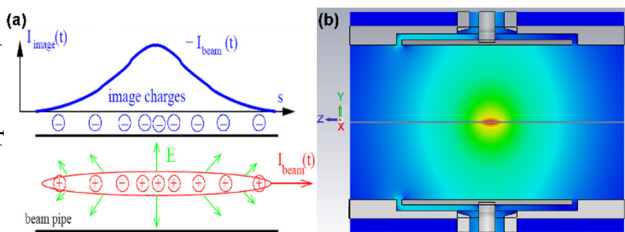
Figure 5: (a) Scheme of induced charges on a metal plate by a charged beam. (b) MYRRHA BPM transversal cut in electrostatic field results of CST with the wakefield solver.

Considering a BPM composed by a perfect electrical conductor, geometry leads to field boundary conditions. We need to study the electrostatic field propagation along the BPM. CST simulations has been done with and without the BPM. Figure 6 compares the transverse electrostatic field function of Y axis for a bunch at Z=0 (see Fig. 5 (b)) with and without BPM.
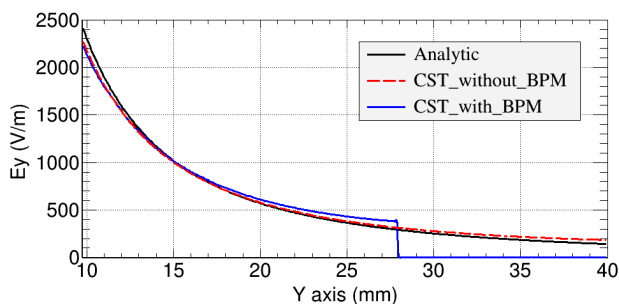

Figure 6: Electrostatic field along the Y axis with BPM (in blue), without BPM (in red dashed line), and from analytic (in black).

The analytical estimation is close to the CST results before and after the electrode position. The electrode in y = 28 mm sets a boundary condition Ey = 0. With the BPM, we see a difference to 100 V/m near the pick-up. The induced charges depend to the electrostatic field propagation, the analytic estimation of the electrostatic field need to consider the BPM geometry.

The repetition rate allows the acquisition chain to digitalize the output signal from the first harmonic (176 MHz) to several harmonics. To quantify these harmonics, a Fast Fourier Transformation (FFT) is applied. We study the signal transmission to the acquisition chain, with a specific frequency behaviour, characterized by its bandwidth. Figure 7 (a) shows the output voltage of the BPM from a centred beam, for different bunch RMS lengths σ_z. The FFT representation illustrates the beam length influence on the signal frequency components (see Fig. 7 (b)). -3dB attenuation from the maximum indicates a high-cut frequency f_{cut}= 1GHz due to the pick-up capacity ($C_{BPM} \sim 3pF$) for a 50 Ω termination. To use the same BPM along the HEBT, the measurement has to be independent form the bunch length extension in the line. The acquisition signal should consider frequencies below 500 MHz. The longitudinal rms size of the beam at the exit of the LINAC is 1.85 mm and about 20 mm at the end of the PTF line.
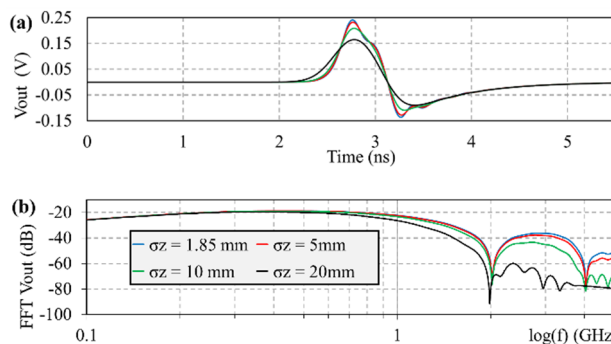

Figure 7: Output voltage from an electrode of the MYRRHA's BPM, for a centred 100 MeV / 4 mA Proton beam. Its temporal representation in V (a) and frequency representation in dB (b).

CONCLUSION

The beam dynamic study of the MINERVA HEBT has been achieved for the MYRTE project. A first modular solution of kicker-septum has been specified. Its adaptability will be improved by adding elements after the septum.

The electrostatic field propagation in the BPM has been calculated analytically and simulated with CST. BPM measurements on real beam will be done at IPHI facility [11], SPIRAL2 [12], MYRRHA. These measurements will confirm the parametrisation of the simulation.

ACKNOWLEDGEMENTS

REFERENCES

[1] D.Vandeplassche, "The MYRRHA Linear Accelerator", in Proc. IPAC'11, San Sebastian, Spain, Sep. 2011, paper WEPS090, pp. 2718-2720.

[2] MINERVA in MYRRHA Phase 1, MYRTE WP2, CERN, Switzerland, October 2018.

[3] H.R. Ravn and B.W. Allardyce, "On-Line Mass Separators", in Treatise on Heavy-Ion Science, Edt. D. A. Bromley, Plenum Press, New York, ISBN 0-306-42949-7, 1989

[4] https://cordis.europa.eu/project/rcn/196919/factsheet/en

[5] TraceWin code: http://irfu.cea.fr/dacm/logiciels/index.php

[6] J. Borburgh and M. Crescenti, "Final Design, Special Magnets", CERN AB Division, Geneva, July 2003.

[7] M. Paraliev, "Septa I & II ", Erice Italy: CERN Accelerator School, March 2017.

[8] J. Borburgh et al., "Design and Development of Kickers and Septa for MedAustron", in Proc. IPAC'10, Kyoto, Japan, May 2010, paper THPEB032, pp. 3954-3956.

[9] Peter Forck, "Beam Position Monitor", GSI, CAS, Darmstadt, Germany, May 2008.

[10] https://www.cst.com/

[11] P-Y. Beauvais et al., "Status Report on the Saclay High-Intensity Proton Injector Project IPHI", in Proc. EPAC'00, Vienna, Austria, Jun. 2000, paper THOAF202, pp. 283-285.

[12] M.-G. Saint Laurent et al., SPIRAL PHASE-II, European RTT, Final report, ERBFMGECT980100, September 2001.